THE JOURNAL OF BIOLOGICAL CHEMISTRY
Vol. 278, No. 46, Issue of November 14, pp. 45999–46006, 2003
Printed in U.S.A.

The Evolutionarily Conserved Trimeric Structure of CutA1 Proteins Suggests a Role in Signal Transduction*[S]

Received for publication, April 28, 2003, and in revised form, August 28, 2003
Published, JBC Papers in Press, August 29, 2003, DOI 10.1074/jbc.M304398200

Fabio Arnesano‡, Lucia Banci‡, Manuela Benvenuti§, Ivano Bertini‡¶, Vito Calderone§, Stefano Mangani§, and Maria Silvia Viezzoli‡

From the ‡Magnetic Resonance Center (CERM) and Department of Chemistry, University of Florence, Via Luigi Sacconi 6, 50019, Sesto Fiorentino, Florence, Italy and §Department of Chemistry, University of Siena, Via Aldo Moro, 53100, Siena, Italy

CutA1 are a protein family present in bacteria, plants, and animals, including humans. *Escherichia coli* CutA1 is involved in copper tolerance, whereas mammalian proteins are implicated in the anchoring of acetylcholinesterase in neuronal cell membranes. The x-ray structures of CutA1 from *E. coli* and rat were determined. Both proteins are trimeric in the crystals and in solution through an inter-subunit β-sheet formation. Each subunit consists of a ferredoxin-like (β1α1β2β3α2β4) fold with an additional strand (β5), a C-terminal helix (α3), and an unusual extended β-hairpin involving strands β2 and β3. The bacterial CutA1 is able to bind copper(II) *in vitro* through His_2Cys coordination in a type II water-accessible site, whereas the rat protein precipitates in the presence of copper(II). The evolutionarily conserved trimeric assembly of CutA1 is reminiscent of the architecture of PII signal transduction proteins. This similarity suggests an intriguing role of CutA1 proteins in signal transduction through allosteric communications between subunits.

CutA1 is a widespread protein of about 12 kDa found in bacteria, plants, and animals, including humans. The protein was originally identified in a gene locus of *Escherichia coli* called *cutA* involved in divalent metal tolerance (1). The *cutA* locus consists of two operons, one containing a single gene encoding a cytoplasmic protein, CutA1, and the other composed of two genes encoding a 50-kDa (CutA2) and a 24-kDa (CutA3) inner membrane proteins. Molecular genetics studies on the *E. coli cutA* locus showed that some mutations lead to copper sensitivity due to its increased uptake (1). However, the specific function of CutA1 in *E. coli* is still unknown. On the other hand recent studies from two independent groups highlighted a possible role of mammalian CutA1 in the anchoring of the enzyme acetylcholinesterase (AChE)[1] in neuronal cell membranes (2, 3). CutA1 does not directly interact with AChE (2), but the CutA1 gene is widely expressed in different regions of the brain with an expression pattern that parallels that of AChE (3). In addition CutA1 copurified with AChE from human caudate nucleus (3). CutA1, thus, might provide an intriguing link between copper tolerance in bacteria and a complex process in the brain of the most evolved organisms. The function of CutA1 in plants is still unknown.

Copper is a transition metal essential to all organisms since it is involved in many redox reactions and in several biological processes (4). Although essential for cellular metabolism, copper is highly toxic when it exceeds cellular needs and accumulates in the cell. Proteins which bind copper are involved in several human neurological pathologies, such as the Menkes and Wilson diseases, the Alzheimer pathology, and the Creutzfeld-Jacob syndrome (5). For this reason, all organisms must have homeostatic mechanisms that allow the intake of the necessary amount of copper, thus preventing its accumulation beyond the level of toxicity (6, 7); these mechanisms are carried out by proteins that specifically bind copper in the cell.

Intriguingly, although CutA1 from several organisms was annotated as a "divalent cation tolerant protein" in GenBank™, it was also suggested to be possibly involved in at least two unrelated processes in bacteria and mammals, thus fulfilling different functions (1, 2). In an attempt to understand this peculiar behavior and unravel its function, we have determined the crystal structure of one representative protein from bacteria (*E. coli* CutA1) and one from mammals (Rat CutA1) and characterized their copper binding properties. The structural arrangement of CutA1 from both organisms shows a striking similarity to the trimeric assembly of signal transduction proteins, called PII (8), which are involved in the nitrogen regulatory response in bacterial cells and eukaryotic chloroplasts (9, 10). In addition, the *E. coli* protein is able to bind a Cu(II) ion in a site structurally equivalent to the ATP binding site in PII proteins (11, 12). The conserved quaternary structure between bacterial and mammalian CutA1 proteins represents an important breakthrough for the comprehension of their function.

EXPERIMENTAL PROCEDURES

Genome Analysis—CutA1 sequences were searched in GenBank™ (www.ncbi.nlm.nih.gov/Entrez) using BLAST (www.ncbi.nlm.nih.gov/BLAST). Conservation was calculated from multiple alignment of CutA1 sequences using MULTALIN (pbil.ibcp.fr). STRING (www.bork.embl-heidelberg.de/STRING) was used to identify possible functional associations between CutA1 and neighboring genes.

Cloning, Expression and Purification of CutA1—Genomic DNA from

* This work has been supported by European Commission Contracts HPRI-CT-2001-50028 and QLG2-CT-2002-00988, European Community Access to European Molecular Biology Laboratory Hamburg Outstation Contract HPRI-CT-1999-00017, and Italian Ministero dell'Università e della Ricerca Scientifica e Tecnologica Project COFIN01. The costs of publication of this article were defrayed in part by the payment of page charges. This article must therefore be hereby marked "*advertisement*" in accordance with 18 U.S.C. Section 1734 solely to indicate this fact.

[S] The on-line version of this article (available at http://www.jbc.org) contains Supplemental Figs. 1 and 2.

The atomic coordinates and structure factors (code 1NAQ (E. coli) and 1OSC (rat CutA1)) have been deposited in the Protein Data Bank, Research Collaboratory for Structural Bioinformatics, Rutgers University, New Brunswick, NJ (http://www.rcsb.org/).

¶ To whom correspondence should be addressed. Tel.: 39-055-4574272; Fax: 39-055-4574271; E-mail: bertini@cerm.unifi.it.

[1] The abbreviations used are: AChE, acetylcholinesterase; EXAFS, extended x-ray absorption fine structure; r.m.s.d., root mean square deviation; XAS, x-ray absorption spectroscopy.

TABLE I
Data collection, MAD phasing and refinement statistics for CutA1 from E. coli and rat

	Data collection statistics				
	E. coli CutA1				Rat CutA1, remote (0.934 Å)
	Peak (1.005231 Å)	Inflex (1.00870 Å)	Remote (0.932 Å)	High resolution remote (0.932 Å)	
Space group	$P2_12_12_1$				
Cell dimensions (Å)	a = 55.44			a = 55.99	a = 70.39
	b = 89.17			b = 89.56	b = 88.27
	c = 121.63			c = 122.30	c = 125.85
Resolution (Å)	40.0–2.0	40.0–2.0	40.0–2.0	40.0–1.7	40–2.15
Total reflections	275,560 (44,905)	276,182 (45,035)	205,853	643,844 (90,452)	300,781 (32,115)
Unique reflections	37,431 (5,921)	37,408 (5,922)	28,532	65,739 (9,337)	46,060 (6,646)
Completeness	91.8 (91.8)	91.8 (91.8)	92.4 (91.6)	97.2 (96.3)	100 (100)
Anomalous completeness	91.6 (90.6)	91.5 (90.5)	92.4 (91.3)	97.1 (96.0)	
R_{sym} (%)	9.8 (32.7)	10.0 (38.1)	9.5 (23.2)	9.1 (51.9)	7.3 (47.0)
R_{anom} (%)	9.5 (15.8)	8.9 (16.1)	7.9 (19.0)	8.0 (26.4)	
Multiplicity	7.3 (7.0)	7.3 (7.3)	7.2 (6.7)	9.7 (9.6)	6.5 (4.8)
$I/\sigma I$	4.3 (2.2)	4.3 (1.9)	4.9 (1.7)	5.7 (1.1)	5.3 (1.7)
	Refinement statistics				
Resolution (Å)			20–1.7		20–2.15
R_{cryst} (%)			20.3		18.9
R_{free} (%)			25.5		26.0
Protein atoms			4,831		5171
Ligands			113		
Water molecules			343		404
B protein (Å^2)			20.4		38.7
B solvent (Å^2)			24.5		51.6
r.m.s.d. bond length (Å)			0.02		0.03
r.m.s.d. bond angles (°)			1.99		2.6
Estimate of the coordinate error based on SigmaA plot (Å)			0.11		0.16

E. coli (strain LE392) was extracted and purified using the DNeasy tissue kit (Qiagen). The plasmid encoding the CutA1 gene from *Rattus norvegicus* was a kind gift of Prof. Eric Krejci.

E. coli strain DH5α was used as the cloning host, and the strain BL21(DE3) Gold was used for protein expression (Stratagene). The expression vector was constructed by amplifying the CutA1 gene from *E. coli* genomic DNA and from rat cDNA through PCR. The primers were designed to introduce NcoI and BamHI sites at either end of the gene to facilitate cloning into the expression vector pET16-b (Novagen). The correct DNA sequences of the obtained plasmids were confirmed by DNA sequencing analysis.

For protein production *E. coli* BL21(DE3) Gold competent cells were transformed with the constructed plasmids and selected with 100 μg/ml ampicillin. *E. coli* cultures were grown aerobically in 2× yeast-tryptone (YT) medium supplemented with 200 μg/ml ampicillin to mid-exponential phase and induced with 0.8 mM isopropyl-β-D-thiogalactopyranoside for 16 h at 37 °C. Cells were harvested, resuspended, and disrupted through sonication (8 cycles, 30 s each). Both proteins were purified through anionic exchange chromatography using a DEAE-Sepharose CL6B (Amersham Biosciences) column equilibrated with 50 mM Tris-HCl, pH 8, and then eluted with two linear gradients (0–0.3 M NaCl in 50 mM Tris, pH 8 (total volume 200 ml), and 0.3–1.0 M NaCl in 50 mM Tris, pH 8 (total volume 900 ml)). Fractions containing the CutA1 proteins and detected through SDS-PAGE were pooled together and concentrated. Both the proteins were obtained in high yield (~150 mg/liter of culture).

Protein Characterization—Electrospray mass spectra were taken with an Applied Biosystems electrospray ionization-time of flight Mariner mass spectrometer. The actual molecular mass was determined by gel filtration chromatography on a Superdex 75 column (Amersham Biosciences) equilibrated with 10 mM phosphate buffer, 100 mM NaCl, pH 7.0. To obtain a calibration line mixtures of various size standards were loaded. Transferrin was used in each mixture to determine the void volume.

^{1}H,^{15}N and ^{1}H,^{13}C heteronuclear single quantum coherence NMR experiments were recorded on a ^{13}C,^{15}N-enriched apoCutA1 sample on Ultra Shield 700 Bruker spectrometer using a triple resonance (TXI) 5-mm probe equipped with pulsed field gradients along the *xyz* axes.

Binding of copper(II) to CutA1 was followed through electronic spectroscopy using a Varian Cary 50 spectrophotometer. Copper content was evaluated through atomic absorption measurements with a PerkinElmer Life Sciences 2380 instrument. X-band EPR spectra were acquired with a magnetic field modulation frequency and amplitude of 100 kHz and 12.00 G, respectively, at 10 K on a BRUKER EMX (9.5 GHz) EPR spectrometer equipped with an ESR 900 helium flow cryostat (Oxford Instruments).

Crystallization of CutA1 from E. coli and Rat—Crystals of CutA1 were grown in a few days using the vapor diffusion technique at 20 °C from about 12 mg/ml *E. coli* and 10 mg/ml rat CutA1 (~1 mM protein solutions). For *E. coli* CutA1, the solution contained 0.1 M Hepes, pH 7.5, 2.0 M $(NH_4)_2SO_4$, 2% PEG 400 (polyethylene glycol), and 3 mM 4-(hydroxymercuri)benzoic acid, and for rat CutA1, the solution contained 0.1 M sodium acetate, pH 4.6, 30% 2-methyl-2,4-pentanediol (MPD), 5 mM $CuSO_4$, 20 mM $CaCl_2$. The crystals of CutA1 both from *E. coli* and from rat were flash-frozen under a cold nitrogen stream at 100 K without the addition of cryoprotectants.

Data Collection and Structure Determination—A 2.1-Å resolution MAD data set at the mercury edge was collected at 100 K on CutA1 from *E. coli* using synchrotron radiation (European Molecular Biology Laboratory PX beamline BW7B at the DORIS storage ring, DESY, Hamburg, Germany). Furthermore, a monochromatic data set at 0.93 Å was collected at the same beamline on a crystal that diffracted up to 1.7 Å resolution. A monochromatic data set at 0.93 Å was collected at 100 K on rat CutA1 using synchrotron radiation (European Synchrotron Radiation Facility ID14–1 beamline, Grenoble, France). The crystals diffracted up to 2.1 Å resolution. All the data sets were processed using MOSFLM 6.2 (13, 14) and scaled with SCALA (14, 15). The phasing on CutA1 from *E. coli* was performed with the program SOLVE (16). The density modification and a partial chain tracing were performed with the program RESOLVE (16). The subsequent exhaustive chain tracing was carried out on the high resolution monochromatic data set with the program ARP/WARP 6.0 (17). The structure of rat CutA1 was solved using the molecular replacement method and the software MOLREP (14, 18); a monomer of CutA1 from *E. coli* was used as the model in the rotation and translation function. The rat CutA1 structure shows some degree of disorder in the loop encompassing residues 82–90. In subunit A the electron density for the side chains of residues Tyr-86 and Glu-87 is very weak, and His-84 appears to be present in at least two conformers. Similar disorder of this loop is present in subunits E and F, which prevents the building of side chains of Tyr-86 and Glu-87 in E and of Glu-87 in F. Both structures were then refined, and water molecules were added using REFMAC5 (14, 19) and CNS (20). Table I shows the data collection and refinement statistics for the two proteins.

The program Xtalview/Xfit (21) was used for molecular rebuilding

and visualization for both structures. The stereochemical quality was assessed using the program PROCHECK (22). The program DALI (23) was used to search the Protein Data Bank for proteins with a similar structure to CutA1.

X-ray Absorption Spectroscopy (XAS) Data Collection and Analysis—XAS data were collected at DESY (Hamburg, Germany) at the European Molecular Biology Laboratory bending magnet beam line D2 using a silicon (111) double monochromator for the measurement at the copper edge, with the DESY storage ring operating under normal conditions (4.5 GeV, 90–140 mA).

The XAS data were recorded by measuring the Cu-Kα fluorescence using a Canberra 13-element solid-state detector over the energy range from 8735 to 9875 eV using variable energy step widths. In the x-ray absorption near edge structure (XANES) and extended x-ray absorption fine structure (EXAFS) regions steps of 0.3 and 0.5–1.2 eV were used, respectively. 10 scans were recorded for a total of more than 1.0/0.6 million counts per experimental point and then averaged. The full, k^3 weighted, EXAFS spectrum (17–750 eV above E_0 and its Fourier transform calculated over the range 3.0–14.0 $Å^{-1}$ were compared with theoretical simulations obtained using the set of programs EXCURVE9.20 (24). The quality of the fit was assessed by the fit function through the parameter ϵ^2 (25) and by the R-factor as defined within EXCURVE9.20 (24).

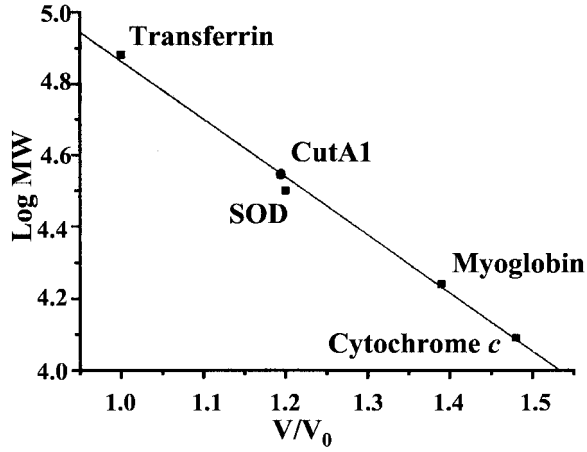

FIG. 1. **Molecular weight (*MW*) determination of CutA1 from *E. coli* through gel filtration chromatography (Superdex 75 column; Amersham Biosciences).** *V*, elution volume of each standard protein or CutA1; V_0, elution volume of transferrin; *SOD*, superoxide dismutase.

RESULTS

Ortholog and Paralog Analysis of CutA1 Sequences—In *E. coli* CutA1 is encoded by one of the three genes of the *cutA* locus, which is involved in tolerance to Cu^{2+} and other heavy metal ions (1). A search of gene data banks located numerous sequences similar to CutA1 from *E. coli* in a large variety of organisms (36 bacteria, 13 Archaea, and 9 eukaryotes). They are reported in Supplemental Fig. 1. The second gene of the *cutA* locus encodes the transmembrane electron transporter CutA2. A gene homologous to CutA2 is found adjacent to CutA1 in a group of bacterial species (*Yersinia pestis*, *Salmonella typhimurium*, *Ralstonia solanacearum*, *Xanthomonas campestris*, *Xanthomonas axonopodis*, *Xylella fastidiosa*). For some of them (*Y. pestis* and *S. typhimurium*) the CutA1 sequence is highly similar to the *E. coli* protein (>60% identity). Moreover, in the same group of organisms a third gene, called CutA3 and belonging to the *cutA* locus, is found next to CutA2. In *E. coli*, CutA1 and CutA2 are in different operons but implicated together in divalent cation tolerance (1). The function of CutA3 is not known, but a search of similar sequences suggests it is a putative transcriptional regulator.

CutA1 also exists in all the eukaryotic genomes sequenced up to now, except yeast, with all the sequences sharing a high degree of identity except in the N-terminal part. In CutA1 of mammals the N-terminal sequence is hydrophobic and might represent either a cleavable secretion signal, a mitochondrial import signal, or a transmembrane anchor (2). The bacterial protein is devoid of this hydrophobic domain, and CutA1 is cytoplasmic in *E. coli*. The rat sequence contains an additional Pro-rich stretch of 12 residues (to which we assign negative residue numbers) at the N terminus, and 6 more residues at the C terminus. Excluding the N-terminal sequence, CutA1 from *E. coli* and rat have 35% residue identity, which increases to 55% when conservative substitutions are considered. Interestingly, in rat and mouse two further genes are present whose sequences are very similar (80% residue identity). These proteins lack the highly conserved Cys-39, which is replaced by a Ser, and share only 40% residue identity with their paralog sequences containing Cys-39.

Protein Characterization—The expressed CutA1 proteins from both organisms turned out soluble and stable for concentrations up to 3 mM in various buffers. The extinction coefficient at 280 nm was determined on the basis of the amino acidic compositions of the proteins and was 17,900 cm^{-1} M^{-1} for *E. coli* and 16,500 cm^{-1} M^{-1} for rat CutA1. The molecular weight, as measured from electrospray mass spectra in denaturing conditions, was 11,841 ± 1 Da for *E. coli* CutA1, corresponding to residues 5–112, and 13,893 ± 1 Da for rat CutA1, corresponding to residues −12 to 118. On the other hand gel filtration chromatography at neutral pH gives an apparent molecular mass of 35,300 ± 400 Da for *E. coli* CutA1, which indicates that the protein is in a trimeric state (Fig. 1). The foldedness and the aggregation state were assessed through ^1H,^{15}N heteronuclear single quantum coherence NMR spectra, which showed well dispersed signals in both dimensions, indicative of a well folded protein (Supplemental Fig. 2). Furthermore, a signal line width analysis carried out on the ^1H,^{15}N heteronuclear single quantum coherence spectrum of CutA1 indicates that line widths are essentially the same for all the signals, with an average value of 32 ± 3Hz, which is comparable with a value of 30 ± 4Hz found for dimeric human Cu,Zn-superoxide dismutase (153 amino acids, ~32 kDa) and different, outside the experimental error, from that of monomeric superoxide dismutase (~16 kDa), which is found to be 17 ± 2 Hz. All these data are consistent beyond any uncertainty with a trimeric state of the protein in solution.

Structure Analysis, a Trimeric Assembly of Ferredoxin-like Subunits—The structure of *E. coli* CutA1 consists of homotrimers displaying approximately a c3v symmetry. In the crystal asymmetric unit, two homotrimers are present that make extensive contacts leading to a dimer of trimers. One trimer is rotated by 60° with respect to the other one around the axis perpendicular to the trimer plane (Fig. 2*A*). The interface between the two trimers is about 3000 $Å^2$, whereas the total interacting surface between each pair of monomers in the trimer is greater than 6000 $Å^2$, giving some evidence that the interactions within the trimer are more specific than those between the two trimers. This is consistent with the observation that in solution the protein exists as a trimer (Fig. 2*C*).

The overall structure of rat CutA1 clearly resembles that of CutA1 from *E. coli*; the space group is the same, and the asymmetric unit contains six subunits in both cases. However, in rat CutA1 the second trimer is rotated by 25° with respect to the first one around the ternary axis (Figs. 2, *B* and *D*). The *a* axis of the cell is about 15 Å larger in the case of rat CutA1, consistent with the rat protein construct having 18 residues more than the *E. coli* protein. However, the longer N terminus in the rat protein cannot be resolved as the interpretable electron density of rat CutA1 crystals starts at residue Gly-3, whereas for *E. coli* CutA1 starts at residue Ser-7. The r.m.s.d. of Cα atoms between *E. coli* and rat proteins as trimers is 0.95

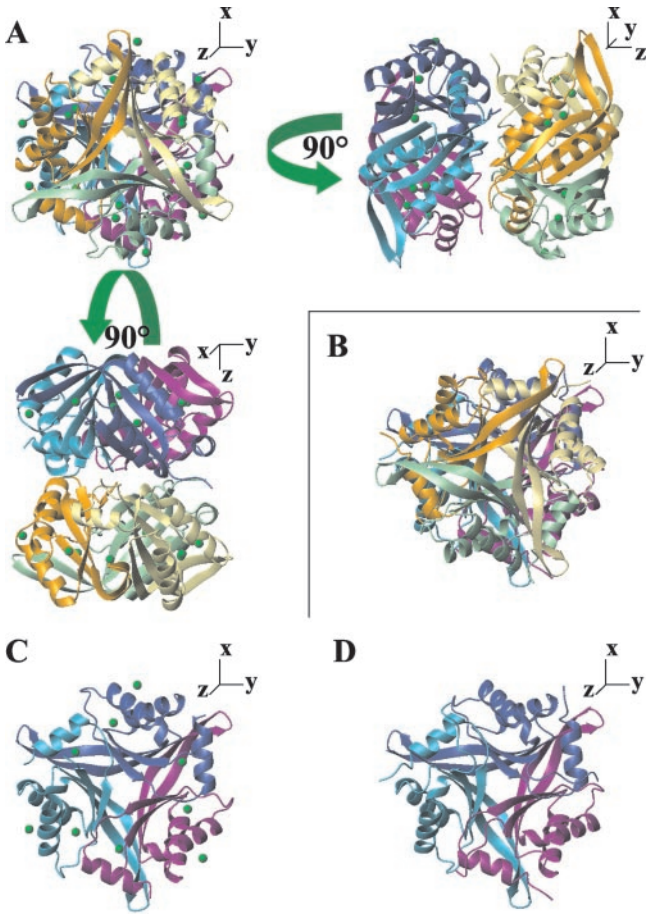

FIG. 2. **Hexameric structures of *E. coli* (*A*) and rat (*B*) CutA1, as found in the crystal asymmetric unit (see "Results" for details), represented as *ribbons*, where each monomer is shown with a different color.** The structure of *E. coli* CutA1 is shown in three different orientations produced by 90° rotations around the *x* and *y* axes. The trimeric structures of *E. coli* (*C*) and rat (*D*) CutA1 are the relevant forms present in solution. Hg(II) ions in *E. coli* CutA1 are represented as *green spheres*.

Å, which confirms a high degree of homology between them, with the larger deviations located in the N- and C-terminal regions.

The following analysis applies to both *E. coli* and rat CutA1. Each monomer exhibits the same overall structure, adopting a ferredoxin-like fold made of an α-β sandwich with antiparallel β-sheet (SCOP classification) (26) and containing an additional short strand (β5) and a C-terminal helix (α3). In the β-sheet, alternate strands are connected by helices with positive cross-overs, resulting in a double $\beta\alpha\beta$ motif where the antiparallel β-sheet packs against antiparallel α-helices. The C-terminal helix packs orthogonal to the N terminus. The β-strands 2 and 3 are connected by an extended β-hairpin (residues Gly-45–Glu-61 in *E. coli* and Ile-46–Glu-60 in rat CutA1) with a Gly at the apex (Gly-54 in *E. coli* and in rat CutA1). The β-hairpin includes a number of residues conserved among all the species (Ser-48, Glu-61, and two aromatic residues, Tyr-50 and Trp-52; residue numbering refers to the *E. coli* CutA1 sequence). Mapping of residue conservation on the structure of the CutA1 monomer, shown in Fig. 3*A*, also highlights a loop region between α2 and β4, spatially close to the β-hairpin and encompassing conserved residues His-84, Tyr-86, and Glu-90. The other highly conserved amino acids are Ala-40 and Cys-39 on β2, Lys-67 on β3, and Trp-106 on α3. These four residues are clustered at the other end of the scaffold.

Least squares superposition of the three *E. coli* CutA1 monomers shows that there are small but significant differences among them, mainly located in the β-hairpin loop (r.m.s.d. of all Cα atoms 0.43–0.56 Å, compared with an estimated error on the coordinates of 0.11 Å). The same occurs for the rat CutA1 monomers (r.m.s.d. of all Cα atoms is 0.32–0.77 Å compared with an estimated error of 0.16 Å). The formation of intersubunit β-sheets is the primary force driving trimer assembly. Hydrogen-bond pairing occurs between the N-terminal half of strand β2 from one subunit and the C-terminal half of strand β2 from another subunit and between strand β4 from one

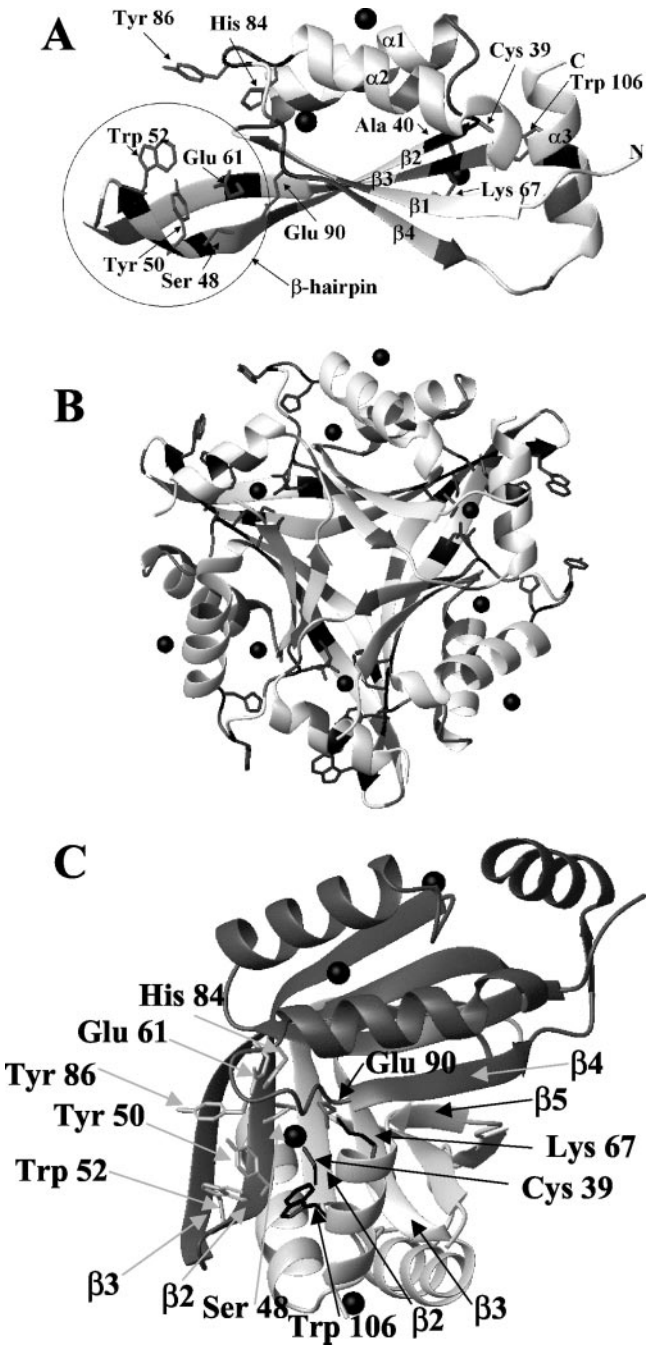

FIG. 3. Mapping of conserved residues on the structure of a monomer (*A*) and a trimer (*B*) of *E. coli* CutA1. Residues conserved in 90% or more aligned sequences are in *black* and are indicated by *arrows*, and residues conserved in 50–90% sequences are in *gray*. *C*, a predicted functional site of CutA1, formed by highly conserved regions of two adjacent monomers are in *white* and *gray*, respectively. Residues conserved in 90% or more aligned sequences and secondary structure elements at the interface between the two monomers are indicated by *arrows*. Hg(II) ions are represented as *black spheres*.

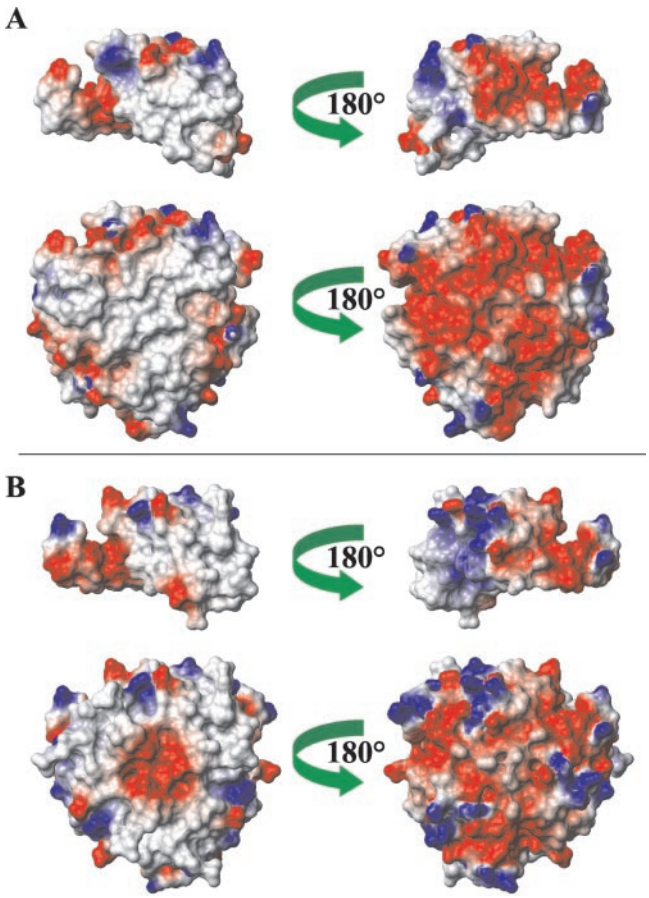

FIG. 4. **Rotated views of the electrostatic surface of *E. coli* (*A*) and rat (*B*) CutA1.** The monomers are shown at the *top* of each *panel*, and the trimers are at the *bottom*. The molecules are oriented as the trimers in Figs. 2, *C* and *D*. The positively, negatively charged and neutral amino acids are represented in *blue*, *red*, and *white*, respectively. The figure was generated with the program MOLMOL (44).

subunit and the short strand β5 from another subunit. These interactions result in three six-stranded anti-parallel β-sheets in the trimer. The β-sheets pack around the 3-fold axis and form 3 concave surfaces (see Fig. 3*B*). The β-hairpin (β2-Loop3-β3) acts as a recognition/oligomerization site because it protrudes from the body of the structure, thus favoring inter-subunit hydrogen bond formation. In addition to the inter-subunit β-sheets, some conserved contacts between two CutA1 subunits (*e.g.* a salt bridge between Lys-67 and Glu-90) stabilize the trimer. The three monomers assemble such that the two highly conserved regions in the monomers are brought together, thus forming three potential functional sites per trimer (Fig. 3, *B* and *C*). A similar trimeric organization is observed in the crystal structure of copper(II)-nitrosocyanin, a trimer of single domain cupredoxins, where each copper center was partially covered by an unusual extended β-hairpin structure from an adjacent monomer (27).

The electrostatic potential surface of the *E. coli* CutA1 monomer is shown in Fig. 4*A*, *top panel*. One face of the protein is largely neutral, whereas the other contains several charged residues producing regions either with negative or positive electrostatic potential. In particular, four Glu residues, also present in the rat protein, produce a large negative potential on the β-hairpin. The rest of the surface shows some scattered negative and positive charges. The trimer-trimer interface is mainly non-polar and hydrophobic, whereas the opposite side of the trimers is negatively charged and exposed to the solvent (Fig. 4*A*, *bottom panel*). The clefts occurring at the trimer interface are lined with conserved acidic residues because they are partially formed by the negatively charged β-hairpins. Sideways, the trimer has a ridge of both positive and negative charges.

In rat CutA1 monomers, the neutral region characterizing one face of the protein is somewhat reduced compared with *E. coli* CutA1. The other face shows a more marked separation between a negative and a positive half, with the latter more extended than in *E. coli* CutA1 (Fig. 4*B*, *top panel*). In the trimer of rat CutA1, the non-polar face has a negative cavity not present in the *E. coli* protein, whereas the other face is entirely charged (Fig. 4*B*, *bottom panel*). As found in *E. coli* CutA1, negative and positive regions from different subunits are in contact, thus stabilizing the trimer through electrostatic interactions throughout its perimeter.

The properties of the electrostatic potential surface of CutA1 trimers suggest very different interaction mechanisms for the apolar face, which interact with the same face of a second trimer, and for the negatively charged face, which is exposed to the solvent. The interaction among the trimers observed in the crystals might mimic a functional property of the hydrophobic surface.

Metal Binding Sites—The ferredoxin-like fold is quite common, present in proteins with different biological functions. This fold is adopted by some metallochaperones, like Atx1, and soluble domains of metal-transporting ATPases (28, 29). An additional C-terminal helix (α3) is characteristic of copper chaperones from plants (10% identity and 65% similarity with CutA1), where it has been postulated to be responsible for the metallochaperone plant-exclusive intercellular transport (30). Despite the fold similarity with copper chaperones and its role in copper tolerance, CutA1 does not possess the classical C*XX*C motif, known to bind Cu(I) in cytosolic metallochaperones. In *E. coli* CutA1 the three cysteines (16, 39, and 79) are far apart both in the sequence and in the structure, none within a single subunit nor in the trimer arrangement. This suggests that potential metal binding features of CutA1 are different from those of metallochaperones (28, 29).

In the *E. coli* CutA1 structure, each Cys binds one mercury atom. Close to two of the three mercury atoms of each monomer there is a His residue; His-83 is close to mercury bound to Cys-79, and His-84 is close to mercury bound to Cys-16. His-83 and His-84 are in adjacent positions, but only His-83 is at true bond distance from the metal; in the third site Glu-90 might interact with mercury bound to Cys-39 of a second monomer.

Only one of the three cysteines (*i.e.* Cys-39) of CutA1 from *E. coli* is fully conserved. The sequence of CutA1 from rat has two Cys residues, *i.e.* Cys-18 (conserved in mammals and corresponding to Cys-16 of *E. coli*) and Cys-39.

Interaction of the CutA1 Protein with Copper; UV-visible, EPR, and EXAFS Analysis of Cu(II)-CutA1—Because of the finding that *E. coli* CutA1 is involved in metal resistance in bacteria, it was proposed that CutA1 might bind transition metal ions (1). We have, therefore, characterized the interaction of the *E. coli* CutA1 apoprotein with Cu(II).

When the apoprotein is titrated with increasing amounts of Cu(II) the electronic spectrum changes, with the formation of absorption bands at 27,400 cm^{-1} and 16,800 cm^{-1} nm, whose intensity increases as the Cu(II) concentration increases. From the pattern of the absorption bands an affinity constant of $1.07 \pm 0.5 \times 10^4$ M^{-1} can be estimated. The EPR spectrum provides $g = 2.21$, $g_{\perp} = 2.07$, and $A = 180 \times 10^{-4}$ cm^{-1}.

The electronic spectrum is characteristic of a type 2 copper site (31); the band at 27,400 cm^{-1} can be assigned to a sulfur-to-Cu(II) charge transfer transition on the basis of the high extinction coefficient ($\epsilon = 1600$ cm^{-1} M^{-1}), whereas the weaker

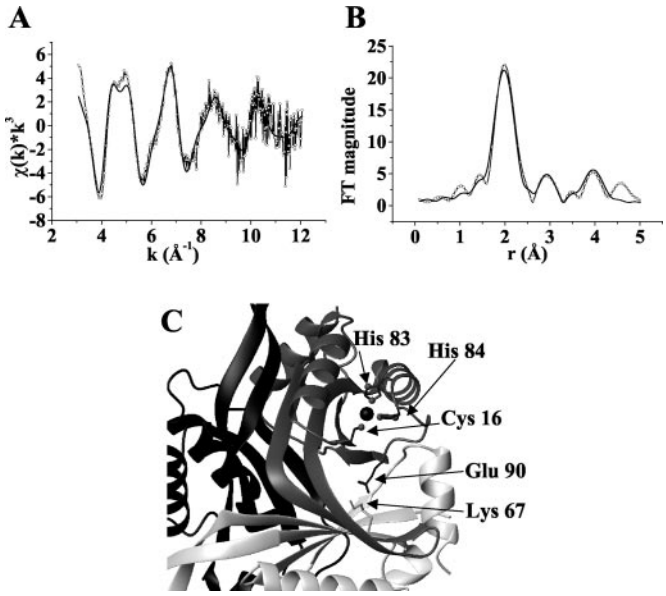

FIG. 5. **Experimental (*solid line*) and simulated (*open circles*) EXAFS spectrum of *E. coli* Cu(II)-CutA1 (*A*) and its Fourier Transforms (*B*); *C*, modeling of the Cu(II) binding site on the structure of *E. coli* CutA1.** The potential site for copper binding is shown as a *black sphere*, and the potential ligands are indicated. The side chains of Glu-90 of one monomer (in *dark gray*) and Lys-67 of the adjacent monomer (in *light gray*), which form an inter-subunit salt bridge, are also shown.

band at 16,800 cm^{-1} can be due to a d-d transition (31, 32). This type of coordination is also fully consistent with the EPR parameters. Similar electronic and EPR spectra have been recently observed in Cu(II) complexes with peptides and have been assigned to a Cu(II)-N_2SX chromophore in a square planar environment (33). Rat CutA1 was titrated with Cu(II) in the same way as *E. coli* CutA1, but even a small addition of Cu(II) induced protein precipitation.

Attempts to crystallize *E. coli* CutA1 in presence of Cu(II) ions have been so far unsuccessful. Soaking of the mercury-derivatized crystals in Cu(II) solutions did not produce Cu(II) adducts of the protein, as shown by the electron density maps.

To ascertain the nature of the ligands involved in copper binding to *E. coli* CutA1 we measured x-ray absorption spectra of the Cu(II)-CutA1 1:1 complex in solution. The EXAFS spectrum and its Fourier transform are reported in Fig. 5, *A* and *B*, respectively. The data show that Cu(II) is bound to two histidines at an average distance of 1.91 (2) Å, one O/N ligand at 1.96 (2) Å, and one cysteine sulfur at 2.16 (2) Å in a square planar geometry (see Table II). Comparison of the EXAFS and crystallographic results suggests that Cu(II) can bind Cys-16 and that, with a little rearrangement of Cys-16 and a minor variation of the χ_1 dihedral angles of His-83 and His-84, these residues can form a metal binding site with a geometry in agreement with EXAFS data (Fig. 5*C*). The fourth N/O ligand found from EXAFS analysis can be either an oxygen from a nearby peptide carbonyl or a water molecule. In support of this latter hypothesis, a water molecule is found in all monomers of *E. coli* CutA1 at about 3.5 Å from Hg(II) bound to Cys-16, indicating that this metal site is solvent-accessible. The fourth ligand could also be an oxygen from the carboxylate group of Glu-90, which is engaged in a salt bridge with Lys-67 of another subunit in the present structure. In this latter hypothesis, Cu(II) binding would break this salt bridge, thus destabilizing the interaction between two adjacent subunits (see Fig. 5*C*).

CutA1 and PII Signal Transduction Proteins Share the Same Trimeric Assembly—The structures of CutA1 from both organisms show that the ferredoxin-like subunits assemble into trimers involving a long β-hairpin (β2-Loop3-β3), which protrudes toward the exterior of the scaffold and which is missing in most of the other proteins sharing this fold. The presence of this unique feature brings to a trimeric assembly of CutA1, which is quite uncommon. A similar architecture can be found in the Protein Data Bank only for members of the superfamily of PII (or GlnB)-like proteins (Protein Data Bank codes 1PIL (8), 2PII (34), and 2GNK (11)).

This similarity is not detected at the sequence level because CutA1 and PII show less than random residue identity even if in a recent bioinformatic study the ortholog group of CutA1 proteins was included in the nitrogen regulatory protein superfamily as an extreme case of sequence-based structure prediction (35).

A structure-based sequence alignment of CutA1 and PII (GlnB) from *E. coli* is reported in Fig. 6*A*. Although residue identity between the aligned sequences is less than 10%, both proteins have a βαββαβ-fold. The only meaningful difference in secondary structure is the presence of a C-terminal β strand in GlnB, which replaces helix α3 of CutA1. In addition, within the sequence of GlnB there is an insertion between strands β2 and β3, which produces a large loop, called loop T. Strands β2 and β3 in CutA1 are longer and form a β-hairpin, which is missing in GlnB. The r.m.s.d. of Cα atoms for all the conserved regions (without gaps) for the two superimposed structures is 4.95 ± 0.04 Å among the monomers and 5.18 Å between the two trimers. These values drop to 2.69 ± 0.02 and 2.93 Å, respectively, when only regions of overlapping secondary structure elements are considered (see Fig. 6, *B* and *C*). In particular, β strands 1–4 in the trimeric structures of CutA1 and GlnB are very well superimposed, with an r.m.s.d. of Cα atoms of 1.18 Å.

PII proteins integrate the signals of intracellular nitrogen and carbon status into the control of enzymes responsible for nitrogen assimilation (9, 10). The trimeric structure in PII has a role in the formation of three ligand binding sites. At low levels of Gln (the nitrogen signal) PII undergoes a post-translational modification (uridylylation on a Tyr or phosphorylation on a Ser in some species) that decreases its affinity for histidine kinase, thus ultimately up-regulating expression of nitrogen assimilation genes, such as glutamine synthase (9, 10). PII proteins also bind synergistically small effector molecules like α-ketoglutarate (the carbon signal) and ATP (9, 10).

In PII proteins loop T, which protrudes from the compact core of the structure, contains the solvent-exposed residue Tyr-51, which undergoes the uridylylation essential for the protein function (Fig. 7). In a structurally similar position, CutA1 proteins contain the conserved Tyr-50 and Ser-48, which lie on the β-hairpin and may represent potential uridylylation and phosphorylation sites, respectively. A distinguishing mark of CutA1 is the presence of a highly conserved Cys residue (Cys-39), not present in PII proteins, which is very close to Tyr-50 from another monomer, thus occupying a critical position at the trimer interface (see Fig. 3*C*). Other conserved residues in CutA1 map in regions corresponding to the three ATP binding sites at the trimer interfaces of PII (11). Most of these residues are located in a loop between α2 and β4 (loop B in PII) and form the potential copper binding site in CutA1 (see Fig. 7). The clefts at the trimer interfaces are positively charged in PII, at variance with CutA1, where many Asp and Glu residues determine a negative surface, possibly reflecting the opposite charge of substrate ligands for the two protein families. The three negatively charged clefts in CutA1 may function as channels to target metal ions and/or other cationic effectors to the interior of the protein structure. Despite specific local differences both

TABLE II
Fitting results of the EXAFS spectrum of E.coli Cu(II)-CutA1

The sample is in 100 mM phosphate buffer at pH 7.0. The precision of the structural parameters obtained from the least squares covariance matrix is reported in parentheses. The bond length accuracy can be estimated to 0.02 Å.

Ligand	Distance	DW factor	EF	Fit index	*R*-Factor
	Å	$2\sigma^2 \times 10^3$ *Å*^{2}	*eV*		
2 N-His	1.91 (1)	9 (2)	−3.0	0.8	0.39
1 N/O	1.96 (4)	4 (1)			
1 S-Cys	2.16 (1)	18 (3)			

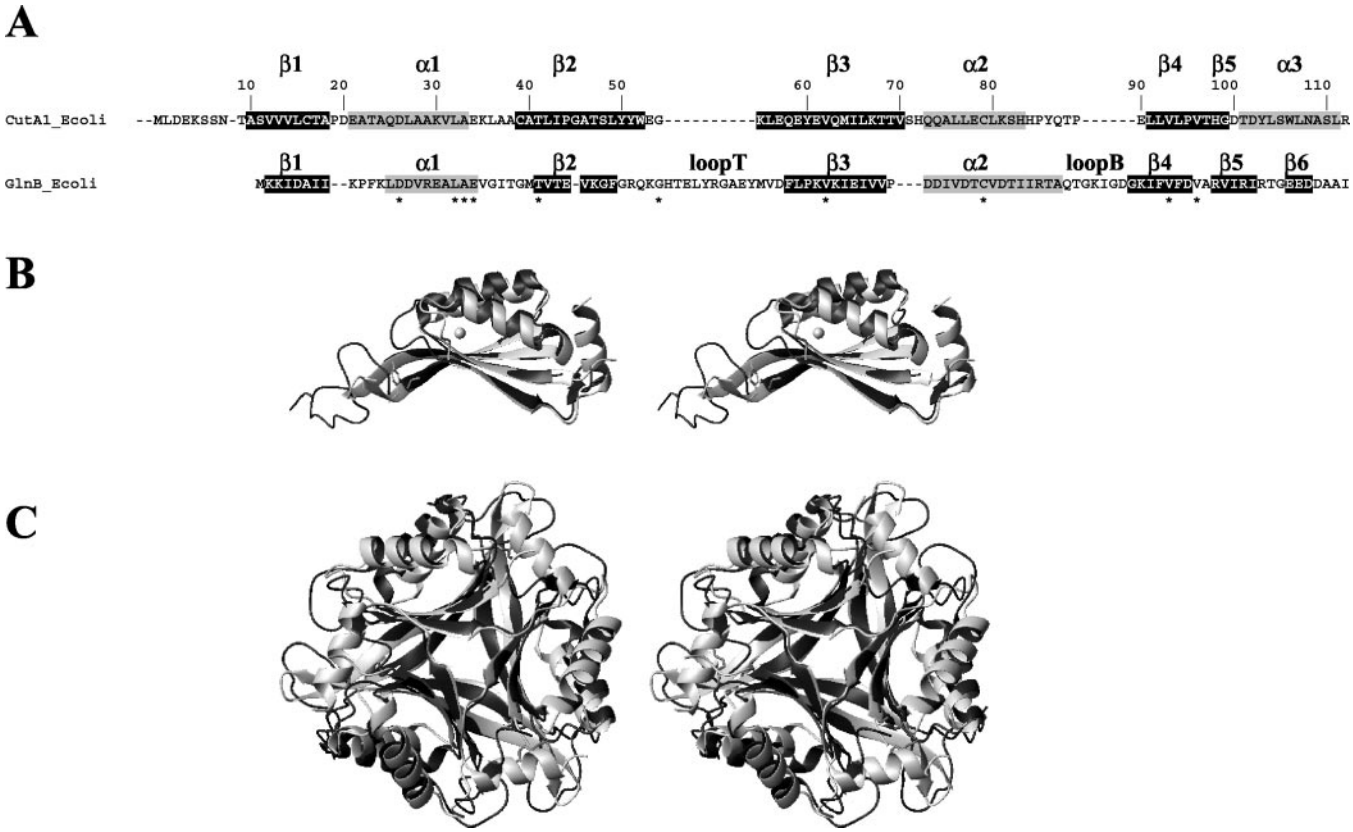

FIG. 6. *A*, structure-based sequence alignment of CutA1 and PII(GlnB) from *E. coli*. Residue numbering refers to the sequence of *E. coli* CutA1. Secondary structure elements are indicated *above* each sequence. Residues belonging to β strands are *shaded* in *black*, and residues in α helices are *shaded* in *light gray*. Conserved residues are indicated with a *star below* the *sequence alignment*. Shown is a stereoview of superimposed structures of monomers (*B*) and trimers (*C*) of *E. coli* CutA1 (in *light gray*) and GlnB (Protein Data Bank code 2PII in *dark gray*). The *white sphere* indicates the potential site for copper binding.

families of proteins share the same quaternary structure, which produces similar binding sites for small ligands at the interface between monomers, which might induce structural changes, thus regulating complex biological processes.

DISCUSSION

E. coli and rat CutA1 structures suggest a general oligomer assembly of the protein that may be essential for protein function. These structural features can be extended to other members of the family on the basis of sequence identity, which for mammalian proteins is larger than 80%.

In *E. coli*, CutA1 was proposed to be implicated in divalent cation tolerance in cooperation with CutA2 (1). In mammalian brain CutA1 is found from biochemical analysis to be involved in the stabilization of the complex between AChE, which regulates cholinergic stimulation (2, 3), and its Pro-rich membrane anchor (PRiMA) at the cell surface (36). Although the protein CutA1 is found to be involved in at least two unrelated processes in bacteria and mammals, the evolutionarily conserved trimeric assembly points to a similar mechanism of action.

In *E. coli* CutA1 may have a sensing/regulatory role and may decrease concentration of excess copper ions in the cell either by direct copper binding, by affecting the import/export of copper ions through the interaction with membrane transporters, or by both mechanisms. It is known that CutA2 (also called DsbD) is involved in a disulfide bond cascade, which carries electrons (reducing equivalents) from the cytoplasm to the periplasm (37). Reduced CutA2 specifically interacts with the oxidized form of the three known periplasmic substrate proteins, DsbC, DsbG, and DsbE, reducing their active sites (38, 39). DsbC and its homolog DsbG are the primary catalysts of incorrect disulfide bond rearrangement during oxidative protein folding. CutA2 is also required for the biogenesis of *c*-type cytochromes in the periplasm, where it transfers electrons to the thioredoxin DsbE (40). Molecular genetics studies showed that the *cutA* locus is not specific for copper, but it also affects levels of Zn^{2+}, Ni^{2+}, Co^{2+}, and Cd^{2+} (1). The absence of metal specificity further supports an upstream role of CutA1 in cooperation with disulfide oxidoreductases like CutA2, *e.g.* in the modulation of the redox state of thiol groups of metal binding C*XX*C motifs, which are found in Cu(I)-ATPases as well as in

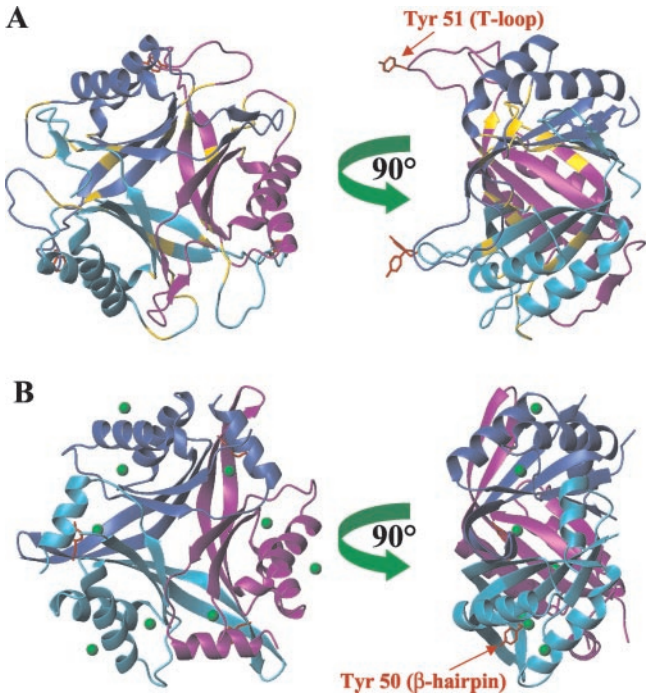

FIG. 7. **Comparison between the trimeric assembly of PII-(GlnB) proteins (Protein Data Bank code 2PII) (*A*) and *E. coli* CutA1 (*B*).** The functionally important Tyr-51 of GlnB is shown in *red* as well as the conserved Tyr-50 on the β-hairpin of CutA1. Residues forming the ATP binding pocket in GlnB are indicated in *yellow*. Hg(II) ions of *E. coli* CutA1 are represented as *green spheres*.

Zn(II)/Cd(II)-ATPases (28). Alternatively, CutA1 could sense cellular levels of different effectors. These effectors may modulate the interaction of CutA1 with different protein partners through allosteric structural changes.

In mammals, AchE is anchored to the membrane in interneuronal synapses through the Pro-rich membrane anchor (PriMA), which contains among others an N-terminal extracellular Pro-rich domain with five Cys residues (36). It was proposed that four Cys residues of this latter domain may organize AChE into tetramers at the surface of neuronal cells by forming disulfide bonds with the C-terminal Cys of AChE (41). CutA1 does not directly interact with AChE (2) but may serve in the electron pathway as sensor/modulator of the redox state of thiol groups of the Pro-rich membrane anchor (PRiMA). In both schemes, the thiol group of Cys-39, highly conserved in the CutA1 family, may have a pivotal role in protein function.

The strong structure similarity of CutA1 with PII proteins might point to an intriguing role of CutA1 in signaling through allosteric communication between monomers. *E. coli* encodes two PII paralog proteins, GlnK and GlnB (11, 34), which can form heterotrimers *in vivo* for fine tuning of the nitrogen signal cascade (42). Interestingly, deuridylylated GlnK binds to the membrane in *E. coli* and acts as a negative regulator of the ammonium transport activity (43). It was suggested that membrane sequestration of GlnK by ammonium transporters (Amt) is a rationale for the trigonal symmetry of these interacting proteins, which are both trimeric (43).

In conclusion, it may be suggested that CutA1 is involved in the tuning of a disulfide bond cascade in bacteria and mammals, acting as the PII proteins do in the nitrogen signal cascade in bacteria and plants. In both cases signal transduction can be achieved through trimer formation, which allows the allosteric communications between distant functional sites and the interaction with membrane transporters.

Acknowledgments—We thank Monica De Stefanis for preparing CutA1 samples and the European Molecular Biology Laboratory and European Synchrotron Radiation Facility beamline staff for access to the facilities. We also thank Prof. Eric Krejci (Ecole Normale Supérieure, Paris) for providing the gene for rat CutA1 and Prof. Anthony Wedd (University of Melbourne, Australia) for helpful discussions and suggestions.

REFERENCES

1. Fong, S. T., Camakaris, J., and Lee, B. T. (1995) *Mol. Microbiol.* **15,** 1127–1137
2. Perrier, A. L., Cousin, X., Boschetti, N., Haas, R., Chatel, J. M., Bon, S., Roberts, W. L., Pickett, S. R., Massoulie, J., Rosenberry, T. L., and Krejci, E. (2000) *J. Biol. Chem.* **275,** 34260–34265
3. Navaratnam, D. S., Fernando, F. S., Priddle, J. D., Giles, K., Clegg, S. M., Pappin, D. J., Craig, I., and Smith, A. D. (2000) *J. Neurochem.* **74,** 2146–2153
4. Linder, M. C. (1991) *Biochemistry of Copper*, pp. 1–13, Plenum Press, New York
5. Bush, A. I. (2000) *Curr. Opin. Chem. Biol.* **4,** 184–191
6. Rosenzweig, A. C., and O'Halloran, T. V. (2000) *Curr. Opin. Chem. Biol.* **4,** 140–147
7. Pena, M. M. O., Lee, J., and Thiele, D. J. (1999) *J. Nutr.* **129,** 1251–1260
8. Cheah, E., Carr, P. D., Suffolk, P. M., Vasudevan, S. G., Dixon, N. E., and Ollis, D. L. (1994) *Structure* (*Lond.*) **2,** 981–990
9. Ninfa, A. J., and Atkinson, M. R. (2000) *Trends Microbiol.* **8,** 172–179
10. Arcondeguy, T., Jack, R., and Merrick, M. (2001) *Microbiol. Mol. Biol. Rev.* **65,** 80–105
11. Xu, Y., Cheah, E., Carr, P. D., van Heeswijk, W. C., Westerhoff, H. V., Vasudevan, S. G., and Ollis, D. L. (1998) *J. Mol. Biol.* **202,** 149–165
12. Xu, Y., Carr, P. D., Huber, T., Vasudevan, S. G., and Ollis, D. L. (2001) *Eur. J. Biochem.* **268,** 2028–2037
13. Leslie, A. G. W. (1991) in *Crystallographic Computing V* (Moras, D., Podjarny, A. D., and Thierry, J.-C., eds) pp. 50–61, Oxford University Press, Oxford
14. Collaborative Computational Project 4 (1994) *Acta Crystallogr. Sect. D* **50,** 760–763
15. Evans, P. R. (1997) *Joint CCP4 and ESF-EACBM Newsletter* **33,** 22–24
16. Terwilliger, T. C., and Berendzen, J. (1999) *Acta Crystallogr. Sect. D* **55,** 849–861
17. Perrakis, A., Morris, R. J. H., and Lamzin, V. S. (1999) *Nat. Struct. Biol.* **6,** 458–463
18. Vagin, A., and Teplyakov, A. (1997) *J. Appl. Crystallogr.* **30,** 1022–1025
19. Murshudov, G. N., Vagin, A. A., and Dodson, E. J. (1997) *Acta Crystallogr. Sect. D* **53,** 240–255
20. Brunger, A. T., Adams, P. D., Clore, G. M., DeLano, W. L., Gros, P., Grosse-Kunstleve, R. W., Jiang, J. S., Kuszewski, J., Nilges, M., Pannu, N. S., Read, R. J., Rice, L. M., Simonson, T., and Warren, G. L. (1998) *Acta Crystallogr. Sect. D Biol. Crystallogr.* **54,** 905–921
21. McRee, D. E. (1999) *J. Struct. Biol.* **125,** 156–165
22. Laskowski, R. A., MacArthur, M. W., Moss, D. S., and Thornton, J. M. (1993) *J. Appl. Crystallogr.* **26,** 283–291
23. Holm, L., and Sander, C. (1996) *Science* **273,** 595–603
24. Binsted, N., and Hasnain, S. S. (1996) *J. Synchrotron Rad.* **3,** 185–196
25. Lytle, F. W., Sayers, D. E., and Stern, E. A. (1989) *Phys. Rev. B* **11,** 2795–2801
26. Lo Conte, L., Ailey, B., Hubbard, T. J., Brenner, S. E., Murzin, A. G., and Chothia, C. (2000) *Nucleic Acids Res.* **28,** 257–259
27. Lieberman, R. L., Arciero, D. M., Hooper, A. B., and Rosenzweig, A. C. (2001) *Biochemistry* **40,** 5674–5681
28. Arnesano, F., Banci, L., Bertini, I., Ciofi-Baffoni, S., Molteni, E., Huffman, D. L., and O'Halloran, T. V. (2002) *Genome Res.* **12,** 255–271
29. Banci, L., and Rosato, A. (2003) *Acc. Chem. Res.* **36,** 215–221
30. Mira, H., Vilar, M., Perez-Paya, E., and Penarrubia, L. (2001) *Biochem. J.* **357,** 545–549
31. Lever, A. B. P. (1984) *Inorganic Electronic Spectroscopy*, Elsevier Science Publishers B. V., Amsterdam
32. Lu, Y., Roe, J. A., Bender, C. J., Peisach, C. J., Banci, L., Bertini, I., Gralla, E. B., and Valentine, J. (1996) *Inorg. Chem.* **35,** 1692–1700
33. Daugherty, R. G., Wasowicz, T., Gibney, B. R., and DeRose, V. J. (2002) *Inorg. Chem.* **41,** 2623–2632
34. Carr, P. D., Cheah, E., Suffolk, P. M., Vasudevan, S. G., Dixon, N. E., and Ollis, D. L. (1996) *Acta Crystallogr. Sect. D* **52,** 93–104
35. Kinch, L. N., and Grishin, N. V. (2002) *Proteins Struct. Funct. Genet.* **48,** 75–84
36. Perrier, A. L., Massoulie, J., and Krejci, E. (2002) *Neuron* **33,** 275–285
37. Katzen, F., and Beckwith, J. (2000) *Cell* **103,** 769–779
38. Krupp, R., Chan, C., and Missiakas, D. (2003) *J. Biol. Chem.* **276,** 3696–3701
39. Haebel, P. W., Goldstone, D., Katzen, F., Beckwith, J., and Metcalf, P. (2002) *EMBO J.* **21,** 4774–4784
40. Edeling, M. A., Guddat, L. W., Fabianek, R. A., Thony-Meyer, L., and Martin, J. L. (2002) *Structure* (*Lond.*) **10,** 973–979
41. Roberts, W. L., Doctor, B. P., Foster, J. D., and Rosenberry, T. L. (1991) *J. Biol. Chem.* **266,** 7481–7487
42. van Heeswijk, W. C., Wen, D., Clancy, P., Jaggi, R., Ollis, D. L., Westerhoff, H. V., and Vasudevan, S. G. (2000) *Proc. Natl. Acad. Sci. U. S. A.* **97,** 3942–3947
43. Coutts, G., Thomas, G., Blakey, D., and Merrick, M. (2002) *EMBO J.* **21,** 536–545
44. Koradi, R., Billeter, M., and Wüthrich, K. (1996) *J. Mol. Graphics* **14,** 51–55

The Evolutionarily Conserved Trimeric Structure of CutA1 Proteins Suggests a Role in Signal Transduction

Fabio Arnesano, Lucia Banci, Manuela Benvenuti, Ivano Bertini, Vito Calderone, Stefano Mangani and Maria Silvia Viezzoli

J. Biol. Chem. 2003, 278:45999-46006.
doi: 10.1074/jbc.M304398200 originally published online August 29, 2003
